Modeling and Optimization of Sub-Wavelength Grating Nanostructures on Cu(In,Ga)Se_2 Solar Cell

2012 Jpn. J. Appl. Phys. 51 10NC14

(http://iopscience.iop.org/1347-4065/51/10S/10NC14)

Japanese Journal of Applied Physics **51** (2012) 10NC14 **REGULAR PAPER**
http://dx.doi.org/**10.1143/JJAP.51.10NC14**

Modeling and Optimization of Sub-Wavelength Grating Nanostructures on Cu(In,Ga)Se_2 Solar Cell

Shou-Yi Kuo[1], Ming-Yang Hsieh[1], Fang-I Lai[2,3*], Yu-Kuang Liao[4], Ming-Hsuan Kao[2,5], and Hao-Chung Kuo[5]

[1]*Department of Electronic Engineering, Chang Gung University, Taoyuan 333, Taiwan*
[2]*Department of Photonics Engineering, Yuan-Ze University, Chungli 32003, Taiwan*
[3]*Advanced Optoelectronic Thechnology Center, National Cheng Kung University, Tainan 701, Taiwan*
[4]*Department of Electrophysics, National Chiao Tung University, Hsinchu 300, Taiwan*
[5]*Institute of Electro-Optical Engineering, National Chiao Tung University, Hsinchu 300, Taiwan*

Received December 10, 2011; accepted February 24, 2012; published online October 22, 2012

In this study, an optical simulation of Cu(In,Ga)Se_2 (CIGS) solar cells by the rigorous coupled-wave analysis (RCWA) method is carried out to investigate the effects of surface morphology on the light absorption and power conversion efficiencies. Various sub-wavelength grating (SWG) nanostructures of periodic ZnO:Al (AZO) on CIGS solar cells were discussed in detail. SWG nanostructures were used as efficient antireflection layers. From the simulation results, AZO structures with nipple arrays effectively suppress the Fresnel reflection compared with nanorod- and cone-shaped AZO structures. The optimized reflectance decreased from 8.44 to 3.02% and the efficiency increased from 14.92 to 16.11% accordingly. The remarkable enhancement in light harvesting is attributed to the gradient refractive index profile between the AZO nanostructures and air.

1. Introduction

The transparent conductive oxide (TCO) layer is important and widely used in thin-film solar cells. Particularly, aluminum-doped zinc oxide (AZO) is a promising alternative material for application as a window layer, mainly due to its low cost, thermal stability, and non toxicity.[1–5] Meanwhile, antireflection coatings (ARCs) play an important role in enhancing the light trapping by minimizing the Fresnel reflection loss at the interface between air and AZO.[6–10] Even though single-layer or multilayer thin-film ARCs have been used, they still have some disadvantages such as material selection, thermal expansion mismatch, and interfacial instability in the thin-film stacks.[11,12] A sub-wavelength periodic nanostructure not only produces a gradient refractive index profile between the AZO and air, but also provides good thermal stability and durability.[13,14]

Thin-film Cu(In,Ga)Se_2 (CIGS) solar cells promise to be the next-generation of photovoltaic devices, since CIGS solar cells have major potential as a source of low-cost, high-efficiency solar electricity, and its efficiency has reached above 20.3%.[15–20] Highly efficient solar cell devices normally consist of a thin buffer layer of CdS deposited onto a CIGS absorber layer, and a highly resistive ZnO layer was introduced between the CdS and ZnO:Al to prevent leakage current.[21–23] To further improve the conversion efficiency, the antireflection function of the surface with sub-wavelength grating (SWG) nanostructure has been investigated technique.[24–32]

To the best of our knowledge, however, there have been no detailed investigations on CIGS solar cells with AZO periodic SWG nanostructures. In this work, we use the rigorous coupled-wave analysis (RCWA) method to simulate the antireflection characteristics of three periodic SWG nanostructures — nanorod arrays (NRs), nanocone arrays (NCs), and nanonipple arrays (NNs) on AZO/ZnO/CdS/CIGS/Mo/glass, as shown in Fig. 1. The electrical and optical properties of AZO SWG structures with various shapes, thicknesses and sizes have been studied.

*E-mail address: filai@saturn.yzu.edu.tw

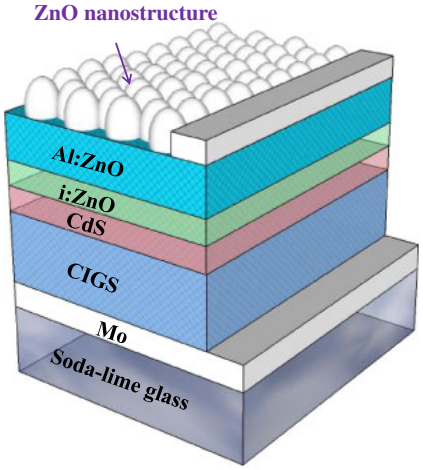

Fig. 1. (Color online) Schematic of CIGS solar cell with AZO nanostructures.

2. Simulation

We analyzed the optical characteristics of CIGS solar cells with SWG nanostructures in a broad spectral range using the RCWA method. The device characteristics of CIGS solar cells are investigated numerically with the APSYS simulation program, which was developed by Crosslight Software Inc. In the simulations, several layers, including a 600-nm-thick AZO transparent conductive oxide layer, a 50-nm-thick intrinsic ZnO layer, a 50-nm-thick CdS buffer layer, a 2-μm-thick CIGS absorber layer, a 500-nm-thick Mo bottom contact, and a glass substrate comprise the CIGS solar cell structure. First, we depict three nanostructure arrays: rod, cone, and nipple on the cell. Then, the AZO periodicity was fixed to optimize the bottom radius and height of the AZO SWG structure. Furthermore, omnidirectional antireflection characteristics were investigated with the incident angle varied from −70 to 70°. Table I shows the basic parameters of the AZO, intrinsic ZnO, CdS, and CIGS layers for the simulations. Besides, all the simulations were performed under an AM 1.5 G light spectrum, and the initial thickness of the AZO film was set to be 600 nm. For comparison, the

Table I. Base simulation parameters for CIGS solar cell. ε, dielectric constant; μ_n, electron mobility; μ_p, hole mobility; N_A, effective density of states in conduction band; N_D, effective density of states in valence band; E_g, band gap energy, and χ, electron affinity.

	AZO	i-ZnO	CdS	CIGS
Thickness (nm)	600	50	50	2000
ε	9	9	10	13.6
μ_n ($cm^2\,V^{-1}\,s^{-1}$)	50	50	10	300
μ_p ($cm^2\,V^{-1}\,s^{-1}$)	5	5	1	30
N_A (cm^{-3})	0	0	0	8×10^{16}
N_D (cm^{-3})	3×10^{20}	5×10^{17}	1×10^{17}	0
E_g (eV)	3.3	3.3	2.4	1.2
χ (eV)	4	4	3.75	3.89

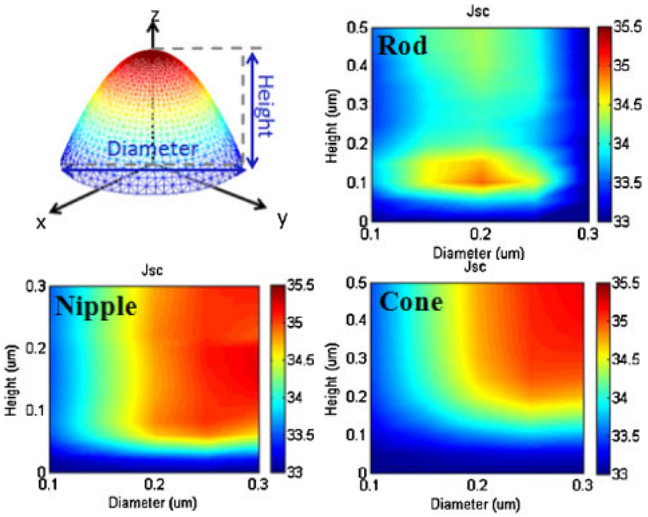

Fig. 2. (Color online) Short-circuit current density of CIGS solar cells with various AZO SWG nanostructures.

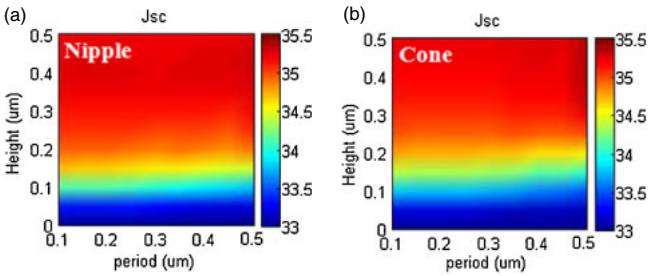

Fig. 3. (Color online) Contour plots for the calculated short-circuit current density as a function of the periods and heights of CIGS solar cells with close-packed (a) nanonipple and (b) nanocone patterns.

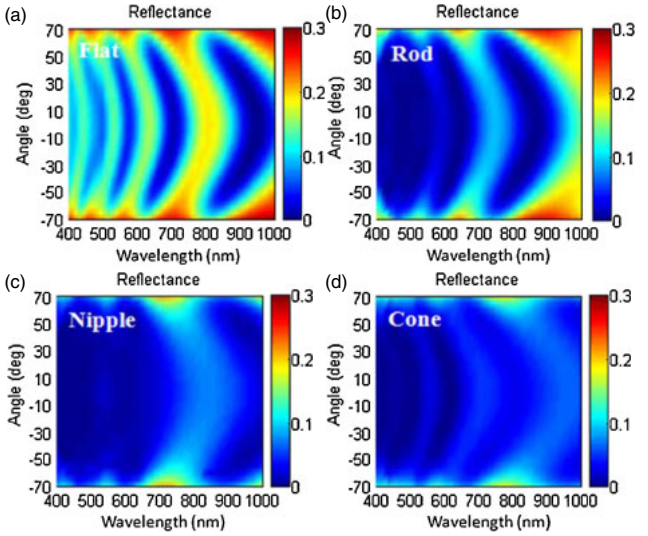

Fig. 4. (Color online) Contour plots for reflectance as a function of the wavelength and incident angle of CIGS solar cells with (a) bare, (b) nanorod-shaped, (c) nipple-shaped, and (d) cone-shaped AZO SWG structures.

total thickness of the AZO nanostructure (rod, nipple, and cone) and underlying AZO film is 600 nm throughout the simulation. To emphasize the dissimilarity of artificial nanostructures, we have that assumed all the interfaces in CIGS solar cells are specular.

3. Results and Discussion

The antireflective properties of AZO films depend strongly on the surface structure. Figure 2 shows the short-circuit current density (J_{sc}) of CIGS solar cells with various AZO SWGs while the period of the AZO SWG structure was fixed at 300 nm. The J_{sc} can be calculated as follows:

$$J_{sc} = \frac{e}{hc}\int_{400nm}^{1000nm} \lambda[1 - R(\lambda)]I_{AM1.5G}\,d\lambda, \qquad (1)$$

where e is the electron charge, h is Planck's constant, $I_{AM1.5G}$ is the intensity of the AM 1.5 G solar spectrum, and the $R(\lambda)$ is the simulated reflectance of the CIGS cell, where the multiple reflection and interference have been taken into account.[33] Moreover, the transmittance is negligible in this case because of the metal bottom contact. We suggest that, therefore, the absorption of photons can be extracted to electrons completely.

From the refractive index variation from air to the AZO film, the rod-shaped nanostructure definitely shows an abrupt change in the effective refractive index. In contrast, the effective refractive indexes of the cone- and nipple-shaped nanostructures change gradually and thus both have similar optical performance. According to the calculation, it is noteworthy that close-packed nanonipple and nanocone patterns have higher J_{sc}, and the AZO SWG nanostructure with 200-nm-thick bottom radius, 100-nm-thick height, 300 nm period has highest J_{sc} (34.8 mA/cm^2). Furthermore, we modulate the period of close-packed nanocone and nanonipple patterns to determine the optimum condition. Figure 3 reveals the close-packed array with a height of 300 nm, and the J_{sc} has reached 35.28 mA/cm^2. In addition, the current density increased only slightly when the height of the SWG nanostructures exceeds 300 nm.

To evaluate the performance of omnidirectional antireflection characteristics, Figs. 4(a)–4(d) show the simulated angle-dependence reflectance of CIGS solar cells with flat and various SWG nanostructures. When the incident was angle increased, the overall reflectance generally increased. Compared with the the flat CIGS solar cell, it is noticeable that the AZO SWG not only shows lower reflectance, but also smaller variations in angle- and wavelength-dependence reflectance.

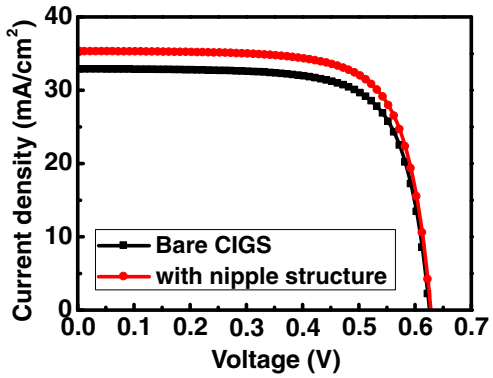

Fig. 5. (Color online) J–V characteristics of bare CIGS solar cell and cell with nipple-shaped SWG structure.

Table II. Photovoltaic parameters of CIGS solar cells with nipple structure and bare cell.

Sample	V_{oc} (V)	J_{sc} (mA/cm^2)	FF	η (%)
Bare CIGS	0.62	32.84	72.64	14.92
Nipple	0.62	35.28	72.7	16.11

Figure 5 shows the photovoltaic current–voltage (J–V) curves of CIGS solar cells with flat and nipple-shaped SWG, and the base parameters are summarized in Table II. From the results, the bare CIGS solar cell and the cell with the nipple-shaped SWG represented average conversion efficiencies (η) of 14.92 and 16.11% with open-circuit voltage (V_{oc}) at ~0.62 V, J_{sc} values of 32.84 and 35.28 mA/cm^2, and fill factors (FFs) of 72.64 and 72.7%, respectively. The J_{sc} of the CIGS solar cell with the nipple-shaped SWG is higher than that of the bare one, thus the enhancement of photovoltaic efficiency. The extra gain (G_p) in photocurrent is calculated as

$$G_P = \frac{\Delta J_{sc}}{J_{sc}} = \frac{J_{sc}(\text{with SWGs}) - J_{sc}(\text{without SWGs})}{J_{sc}(\text{without SWGs})}. \quad (2)$$

Owing to the enhanced antireflection effects, the extra gains in photocurrent G_p for the CIGS solar cell with nanorod-, cone-, and nipple-shaped SWG are 5.9, 6.7, and 7.4%, respectively. Thus, the CIGS solar cell with the nipple-shaped SWG can reach the conversion efficiency of 16.11% owing to the increase in short-circuit current.

4. Conclusion

In summary, the performance of CIGS solar cells with various AZO SWG nanostructures was simulated by the RCWA method. By using close-packed patterns, the simulation results indicates that the optical reflectance can be suppressed and the short-circuit current density increase accordingly. Under optimum conditions, the conversion efficiency of the CIGS solar cell with the nipple-shaped SWG structure is 16.11%, while that of the flat cell is 14.92%. The 8% enhancement in the conversion efficiency is attributed to the effective antireflection effect due to the gradual change in the refractive index. These results demonstrate that the fabrication of AZO SWG nanostructures is an effective approach to enhance the conversion efficiency of the CIGS solar cells.

Acknowledgement

This work was supported by the Green Technology Research Center of Chang Gung University and the National Science Council (NSC) of Taiwan under contract Nos. NSC97-2112-M-182-004-MY3 and NSC-100-2112-M-182-004.

1) O. Lupan, S. Shishiyanu, V. Ursaki, H. Khallaf, L. Chow, T. Shishiyanu, V. Sontea, E. Monaico, and S. Railean: Sol. Energy Mater. Sol. Cells **93** (2009) 1417.
2) J. P. Kar, S. Kim, B. Shin, K. I. Park, K. J. Ahn, W. Lee, J. H. Cho, and J. M. Myoung: Solid-State Electron. **54** (2010) 1447.
3) S. Y. Kuo, K. C. Liu, F.-I. Lai, J. F. Yang, W. C. Chen, M. Y. Hsieh, H.-I. Lin, and W. T. Lin: Microelectron. Reliab. **50** (2010) 730.
4) K. L. Chopra, S. Major, and D. K. Pandya: Thin Solid Films **102** (1983) 1.
5) T. Minami, K. Oohashi, S. Takata, T. Mouri, and N. Ogawa: Thin Solid Films **193–194** (1990) 721.
6) C. J. Ting, C. F. Chen, and C. P. Chou: Optik **120** (2009) 814.
7) X. Li, Q. Tan, and G. Jin: Optik **122** (2011) 2078.
8) K. Yamada, M. Umetani, T. Tamura, Y. Tanaka, H. Kasa, and J. Nishii: Appl. Surf. Sci. **255** (2009) 4267.
9) C.-H. Lin, H.-L. Chen, W.-C. Chao, C.-I. Hsieh, and W.-H. Chang: Microelectron. Eng. **83** (2006) 1798.
10) Y. J. Lee, D. S. Ruby, D. W. Peters, B. B. McKenzie, and J. W. P. Hsu: Nano Lett. **8** (2008) 1501.
11) S. M. Yang, Y. C. Hsieh, and C. A. Jeng: J. Vac. Sci. Technol. A **27** (2009) 336.
12) S. Walheim, E. Schäffer, J. Mlynek, and U. Steiner: Science **283** (1999) 520.
13) K. Chandra Sahoo, Y. Li, and E. Y. Chang: IEEE Trans. Electron Devices **57** (2010) 2427.
14) S. A. Boden and D. M. Bagnall: Appl. Phys. Lett. **93** (2008) 133108.
15) P. Jackson, D. Hariskos, E. Lotter, S. Paetel, R. Wuerz, R. Menner, W. Wischmann, and M. Powalla: Prog. Photovoltaics **19** (2011) 894.
16) M. A. Green, K. Emery, Y. Hishikawa, and W. Warta: Prog. Photovoltaics **19** (2011) 84.
17) M. A. Contreras, K. Ramanathan, J. AbuShama, F. Hasoon, D. L. Young, B. Egaas, and R. Noufi: Prog. Photovoltaics **13** (2005) 209.
18) M. Yamaguchi: J. Appl. Phys. **78** (1995) 1476.
19) A. Chirilă, S. Buecheler, F. Pianezzi, P. Bloesch, C. Gretener, A. R. Uhl, C. Fella, L. Kranz, J. Perrenoud, S. Seyrling, R. Verma, S. Nishiwaki, Y. E. Romanyuk, G. Bilger, and A. N. Tiwari: Nat. Mater. **10** (2011) 857.
20) I. Repins, M. A. Contreras, B. Egaas, C. DeHart, J. Scharf, C. L. Perkins, B. To, and R. Noufi: Prog. Photovoltaics **16** (2008) 235.
21) S. Shirakata, K. Ohkubo, Y. Ishii, and T. Nakada: Sol. Energy Mater. Sol. Cells **93** (2009) 988.
22) E. Q. B. Macabebe, C. J. Sheppard, and E. E. vanDyk: Physica B **404** (2009) 4466.
23) M. M. Islam, S. Ishizuka, A. Yamada, K. Matsubara, S. Niki, T. Sakurai, and K. Akimoto: Appl. Surf. Sci. **257** (2011) 4026.
24) M. Moharam and T. Gaylord: J. Opt. Soc. Am. **72** (1982) 1385.
25) P. Lalanne: J. Opt. Soc. Am. A **14** (1997) 1592.
26) M. E. Motamedi, W. H. Southwell, and W. J. Gunning: Appl. Opt. **31** (1992) 4371.
27) P. Lalanne and G. M. Morris: Nanotechnology **8** (1997) 53.
28) Y. Kanamori, K. Hane, H. Sai, and H. Yugami: Appl. Phys. Lett. **78** (2001) 142.
29) Y. F. Huang, S. Chattopadhyay, Y. J. Jen, C. Y. Peng, T. A. Liu, Y. K. Hsu, C. L. Pan, H. C. Lo, C. H. Hsu, Y. H. Chang, C. S. Lee, K. H. Chen, and L. C. Chen: Nat. Nanotechnol. **2** (2007) 770.
30) C. H. Chiu, P. Yu, H. C. Kuo, C. C. Chen, T. C. Lu, S. C. Wang, S. H. Hsu, Y. J. Cheng, and Y. C. Chang: Opt. Express **16** (2008) 8748.
31) C. H. Chang, P. Yu, and C. S. Yang: Appl. Phys. Lett. **94** (2009) 051114.
32) P. Yu, C. H. Chang, C. H. Chiu, C. S. Yang, J. C. Yu, H. C. Kuo, S. H. Hsu, and Y. C. Chang: Adv. Mater. **21** (2009) 1618.
33) M. A. Tsai, P. C. Tseng, H. C. Chen, H. C. Kuo, and P. Yu: Opt. Express **19** (2011) A28.